

ELEMENTARY PARTICLES AND FIELDS

Theory

Four-Leptonic Decays of Charged and Neutral B Mesons within the Standard Model

A. V. Danilina^{1),2),3)*} and N. V. Nikitin^{1),2),3)**}

Received December 21, 2017

Abstract—The branching ratios and differential distributions for the four-leptonic decays $B^- \rightarrow \mu^+ \mu^- \bar{\nu}_e e^-$, $B^- \rightarrow e^+ e^- \bar{\nu}_\mu \mu^-$, and $B^- \rightarrow \mu^+ \bar{\nu}_\mu \mu^- \mu^-$ are calculated within the Standard Model. The branching ratios for the rare decays $B_{d,s} \rightarrow e^+ e^- \mu^+ \mu^-$ and $B_{d,s} \rightarrow \mu^+ \mu^- \mu^+ \mu^-$ are estimated. Methods for testing the lepton universality in rare multileptonic decays of charged and neutral B mesons are proposed.

DOI: 10.1134/S1063778818030092

1. INTRODUCTION

Investigation of four-leptonic decays of B mesons open the possibility for precision tests of Standard Model predictions in higher orders of perturbation theory. Decays of this type could potentially be background processes for the decays $B_{d,s} \rightarrow \mu^+ \mu^-$, which are extremely rare because of helicity suppression and which have recently become the subject of vigorous studies at the Large Hadron Collider (LHC, CERN) [1–3] in connection with searches for physics beyond the Standard Model (see, for example, the review article of Fleischer and his coauthors [4] and references therein). The objective of the present study is to calculate the branching ratios for the decays of charged B mesons to three light charged leptons and a neutrino and to explore differential distributions associated with these decays. In addition, various estimates of the branching ratios for the decays of neutral $B_{d,s}$ mesons to four light charged leptons are proposed below.

Within the Standard Model, there are two types of rare multileptonic decays of B mesons. Decays of the first type are forbidden at the tree level. They proceed in higher order of perturbation theory via

penguin and/or box loop diagrams (so-called flavor-changing neutral currents). Such decays include the processes $B_{d,s} \rightarrow \mu^+ \mu^- \mu^+ \mu^-$ and processes analogous to them. Many electromagnetic and weak processes at the tree level are used in decays of the second type to obtain a preset multileptonic final state—for example, the decay $B^- \rightarrow e^+ e^- \bar{\nu}_\mu \mu^-$ and similar processes.

In the Standard Model, the t quark makes a dominant contribution to the loop diagrams for rare B -meson decays [5]. In addition to Standard Model processes, B decay amplitudes are good places to search for deviations from the Standard Model in top-quark interaction with various particles beyond the Standard Model (“nonstandard” particles)—for example, anomalous interactions [6–8]—or involve additional loop contributions from nonstandard particles [9–13]. The second type of rare decays are provided by b – u and b – c quarks interaction. Information about such interactions supplements information obtained in studying the interactions of b and t quarks, including anomalous Wub and Wcb vertices. Therefore, investigation of rare four-leptonic decays of B mesons is an important experimental and theoretical method for testing the Standard Model and its extensions.

In deriving theoretical predictions for rare four-leptonic decays of B mesons, the basic problem lies in simultaneously calculating the dependence of hadron form factors on two 4-momentum transfers squared, q^2 and k^2 , for each dilepton in the decay region. This situation differs drastically from that in the problem of determining hadron form factors in rare semileptonic and leptonic radiative decays of B mesons, where the corresponding hadron form factors depend only on

¹⁾Faculty of Physics, Moscow State University, Moscow, 119991 Russia.

²⁾Skobeltsyn Institute of Nuclear Physics, Moscow State University, Moscow, 119991 Russia.

³⁾Institute for Theoretical and Experimental Physics, National Research Center Kurchatov Institute, Bol’shaya Cherevinskaya ul. 25, Moscow, 117218 Russia.

*E-mail: anna.danilina@cern.ch

**E-mail: Nikolai.Nikitine@cern.ch

the square of one 4-momentum transfer at a fixed value of the second (see, for example, [14, 15]). This situation is also dissimilar to the situation prevalent in the four-leptonic decays of light particles. In the multileptonic decays of light mesons, one can disregard the dependence on the squares of 4-momentum transfers for dileptons, assuming that all hadron form factors are constants. This circumstance simplifies substantially the calculation of respective branching ratios and various differential distributions [16, 17].

To date, none of the rare four-leptonic decays discussed in the present article has been discovered experimentally. However, the LHCb Collaboration has set upper limits on the branching ratios for the decays $B_{d,s} \rightarrow \mu^+ \mu^- \mu^+ \mu^-$ [18, 19].

The present article is organized as follows. In Section 2, we give an explicit expression for the effective Hamiltonian and present basic definitions of the hadron form factors used in the present analysis. In Section 3, we study a general dependence of the amplitude for the $B^- \rightarrow \ell^+ \ell^- \bar{\nu}_{\ell'} \ell'^-$ decays on the dilepton 4-momenta and estimate the values of the branching ratios for the decays. Section 4 contains exact formulas for the decay amplitude $B^- \rightarrow \ell^+ \ell^- \bar{\nu}_{\ell'} \ell'^-$ in the case of $\ell \neq \ell'$, while Section 5 gives the analogous formulas for the case of $\ell \equiv \ell'$. In Section 6, we present numerical results for the decays of charged B mesons to three light charged leptons and a neutrino. In Section 7, we obtain various estimates of the branching ratios for the decay of neutral B mesons to four light charged leptons. The Conclusions summarizes basic results of the present study. Kinematical details of four-lepton decays are considered in the Appendix.

2. EFFECTIVE HAMILTONIAN AND HADRON MATRIX ELEMENTS

The Hamiltonian for the $B^- \rightarrow \ell^+ \ell^- \bar{\nu}_{\ell'} \ell'^-$ four-leptonic decays can be represented in the form

$$\mathcal{H}_{\text{eff}}(x) = \mathcal{H}_W(x) + \mathcal{H}_{\text{em}}(x) + \mathcal{H}_{\text{VMD}}(x). \quad (1)$$

The Hamiltonian for the $b \rightarrow u W^- \rightarrow u \ell^- \bar{\nu}_{\ell}$ transitions is given by

$$\begin{aligned} \mathcal{H}_W(x) = & \frac{G_F}{\sqrt{2}} V_{ub} (\bar{u}(x) \gamma^\mu (1 - \gamma^5) b(x)) \\ & \times (\bar{\ell}(x) \gamma_\mu (1 - \gamma^5) \nu_\ell(x)) + \text{h.c.}, \end{aligned}$$

where $u(x)$ and $b(x)$ are quark fields, $\ell(x)$ and $\nu_\ell(x)$ are lepton fields, G_F is the Fermi constant, V_{ub} is an element of the Cabibbo–Kobayashi–Maskawa matrix, and the matrix γ^5 is defined as $\gamma^5 = i\gamma^0\gamma^1 \times \gamma^2\gamma^3$.

The Hamiltonian for electromagnetic interaction has the form

$$\mathcal{H}_{\text{em}}(x) = e \sum_f Q_f (\bar{f}(x) \gamma^\mu f(x)) A_\mu(x),$$

where the elementary charge $e = |e|$ is normalized by the condition $e^2 = 4\pi\alpha_{\text{em}}$, $\alpha_{\text{em}} \approx 1/137$ being the fine-structure constant; Q_f is the charge of the fermion of flavor f in elementary-charge units; $f(x)$ is the field of such fermions; and $A_\mu(x)$ is the 4-potential of the electromagnetic field.

The Hamiltonian describing the Vector Meson Dominance (VMD) model has the form

$$\mathcal{H}_{\text{VMD}}(x) = \sum_{V_i} \frac{e M_{V_i}^2}{f_{V_i}} V_i^\mu(x) A_\mu(x),$$

where $V_i^\mu(x)$ is the field of a vector meson and M_{V_i} is its mass. The absolute values of the dimensionless coupling constants f_{V_i} for $M_{V_i} \gg m_\ell$ are calculated on the basis of experimental values of $V_i \rightarrow \ell^+ \ell^-$ branching ratios according to the relation

$$\Gamma(V_i \rightarrow \ell^+ \ell^-) = \frac{4\pi}{3} \left(\frac{\alpha_{\text{em}}}{|f_{V_i}|} \right)^2 M_{V_i}. \quad (2)$$

For ρ and ω mesons, the coupling constants f_ρ and f_ω are real and positive.

Hadron matrix elements are defined as

$$\begin{aligned} \langle 0 | \bar{u} \gamma^\mu \gamma^5 b | B^-(M_1, p) \rangle &= i f_{B_u} p^\mu, \\ \langle 0 | \bar{u} \gamma^\mu b | B^{*-}(M_{B^*}, k, \varepsilon) \rangle &= \varepsilon^\mu M_{B^*} f_{B^*}, \\ \langle V(M_2, q, \varepsilon) | \bar{u} \gamma_\mu b | B^-(M_1, p) \rangle \\ &= \frac{2V(k^2)}{M_1 + M_2} \epsilon_{\mu\nu\alpha\beta} \varepsilon^{*\nu} p^\alpha q^\beta, \\ \langle V(M_2, q, \varepsilon) | \bar{u} \gamma_\mu \gamma^5 b | B^-(M_1, p) \rangle \\ &= i \varepsilon^{*\nu} \left[(M_1 + M_2) A_1(k^2) g_{\mu\nu} - \frac{A_2(k^2)}{M_1 + M_2} \right. \\ &\quad \times (p + q)_\mu p_\nu - \frac{2M_2}{k^2} (A_3(k^2) - A_0(k^2)) k_\mu p_\nu \Big], \\ \langle B^{*-}(M_{B^*}, k, \varepsilon) | \bar{b} \gamma^\mu b | B^-(M_1, p) \rangle \\ &= \frac{2V_b(q^2)}{M_1 + M_{B^*}} \epsilon_{\mu\nu\alpha\beta} \varepsilon^{*\nu} p^\alpha k^\beta. \end{aligned} \quad (3)$$

Here, M_1 and p^μ are the B^- -meson mass and 4-momentum, respectively; M_2 and M_{B^*} are the masses of intermediate vector mesons; and ε^μ are their polarizations. The 4-vectors p^μ , q^μ , and k^μ satisfy the conservation law $p^\mu = q^\mu + k^\mu$. The components of the fully antisymmetric tensor $\epsilon^{\mu\nu\alpha\beta}$ are fixed by the condition $\epsilon^{0123} = -1$. Further, $g_{\mu\nu}$ is the metric tensor in Minkowski space, its diagonal elements being $\text{diag} g_{\mu\nu} = (1, -1, -1, -1)$.

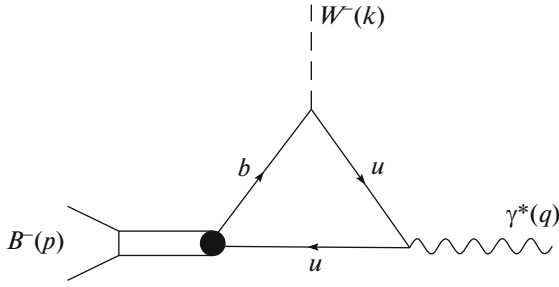


Fig. 1. Diagram involving the emission of a virtual photon from the light quark of the B^- meson and corresponding to the function $G^{(u)}(q^2, k^2, M_{2i}^2)$.

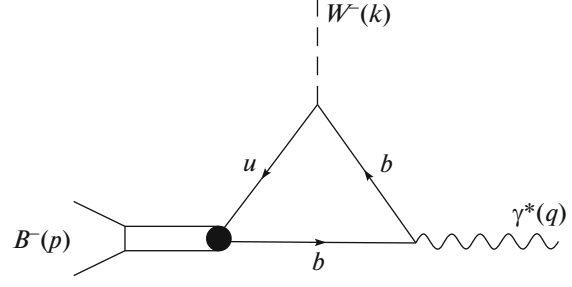


Fig. 2. Diagram corresponding to the function $G^{(b)}(q^2, k^2, M_{B^{*-}}^2)$. Here, a virtual photon is emitted from the heavy quark of the B^- meson.

3. STRUCTURE OF AMPLITUDES AND ESTIMATION OF CONTRIBUTIONS OF VARIOUS DIAGRAMS IN THE APPROXIMATION OF ZERO LEPTON MASSES FOR $B^- \rightarrow \ell^+ \ell^- \bar{\nu}_{\ell'} \ell'^-$ DECAYS

In describing $B^-(p) \rightarrow \ell^+(k_1) \times \ell^-(k_2) \bar{\nu}_{\ell'}(k_3) \ell'^-(k_4)$ decays, there arise diagrams of three types: (1) a virtual photon is emitted by a u quark (see Fig. 1), (2) a virtual photon is emitted by a b quark (see Fig. 2), and (3) bremsstrahlung diagrams in which a virtual photon is described by the lepton ℓ'^- (see Fig. 3).

We denote $q = k_1 + k_2$ and $k = k_3 + k_4$. The general structure of the amplitude corresponding to the diagram in Fig. 1 can be represented as

$$\mathcal{M}_{fi}^{(u)}(q^2, k^2) \sim \sum_i \frac{M_{2i}^2}{q^2} \frac{M_1^2}{q^2 - M_{2i}^2 + i\Gamma_{2i}M_{2i}} \times G^{(u)}(q^2, k^2, M_{2i}^2), \quad (4)$$

where $G^{(u)}(q^2, k^2, M_{2i}^2)$ is a smooth function of the variables q^2 and k^2 , while M_{2i} and Γ_{2i} are, respectively, the masses and widths of intermediate vector mesons containing a $u\bar{u}$ pair. For such states, the amplitude $\mathcal{M}_{fi}^{(u)}(q^2, k^2)$ has Breit–Wigner poles in the variable q^2 . Additionally, there arises a $1/q^2$ pole from the photon propagator. In the limit of $m_\ell \rightarrow 0$, the last pole requires a cutoff at some effective value q_{\min}^2 . The choice of q_{\min}^2 may correspond either to the natural kinematical threshold $4m_\ell^2$, where m_ℓ is a real nonzero mass of the leptons involved in the decay process or to specific kinematical constraints imposed on the momenta of final-state leptons in selecting events in each specific experiment. It is reasonable to choose the natural kinematical threshold at $\ell \equiv \mu$ and to adopt experimental constraints at $\ell \equiv e$.

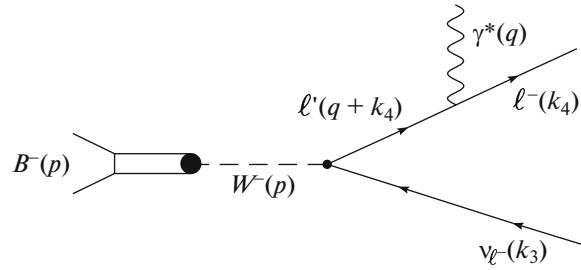


Fig. 3. Diagram corresponding to virtual-photon bremsstrahlung.

The variable k^2 changes over the range of $m_\ell^2 \approx 0 \leq k^2 \leq M_1^2$. The leftmost singularity in the k^2 -variable lies at $k^2 = M_{B^{*-}}^2$. Since $M_{B^{*-}} > M_1$, this singularity lies off the kinematically allowed region of $B^- \rightarrow \ell^+ \ell^- \bar{\nu}_{\ell'} \ell'^-$ decays. The presence of a singularity at the B^{*-} -meson mass is implicitly taken into account in choosing a parametrization of the form factors for the $B \rightarrow \rho$ and $B \rightarrow \omega$ transitions, as is described in detail elsewhere [20].

The amplitude corresponding to the diagram in Fig. 2 can be represented in the form

$$\mathcal{M}_{fi}^{(b)}(q^2, k^2) \sim \frac{M_{B^{*-}} f_{B^{*-}}}{q^2} G^{(b)}(q^2, k^2, M_{B^{*-}}^2), \quad (5)$$

where $G^{(b)}(q^2, k^2, M_{B^{*-}}^2)$ is a smooth function of the variables q^2 and k^2 . In the variable q^2 , the amplitude $\mathcal{M}_{fi}^{(b)}(q^2, k^2)$ has only a pole from the photon propagator in the kinematically allowed region of $4m_\ell^2 \approx 0 \leq q^2 \leq M_1^2$. In just the same way as in the case of the amplitude $\mathcal{M}_{fi}^{(u)}$, this pole requires a cutoff. The next pole in the variable q^2 corresponds to the contribution of the lightest vector meson that has the $b\bar{b}$ quark content (this is the $\Upsilon(1S)$ meson) and whose

mass is nearly twice as high as M_1 , lying off the kinematically allowed region in the variable q^2 . The contribution of $\Upsilon(1S)$ is effectively taken into account in the approximating expression (21) (see below) for the form factor $V_b(q^2)$. In just the same way as the amplitude $\mathcal{M}_{fi}^{(u)}$, the amplitude $\mathcal{M}_{fi}^{(b)}$ does not have singularities in the variable k^2 .

The bremsstrahlung amplitude $\mathcal{M}_{fi}^{(\text{brem})}(q^2, k^2)$, to which the diagram in Fig. 3 corresponds, has only one pole in the variable q^2 from the photon propagator; that is,

$$\mathcal{M}_{fi}^{(\text{brem})}(q^2, k^2) \sim \frac{1}{q^2} G^{(\text{brem})}(q^2, k^2), \quad (6)$$

where $G^{(\text{brem})}(q^2, k^2)$ is a smooth function of the variables q^2 and k^2 . In just the same way as for the amplitudes $\mathcal{M}_{fi}^{(u)}$ and $\mathcal{M}_{fi}^{(b)}$, this pole requires introducing a cutoff procedure in the limit of zero lepton masses. In the variable k^2 , the amplitude $\mathcal{M}_{fi}^{(\text{brem})}$ does not have poles in the kinematically allowed region.

Now we estimate the contributions of each of the three types of diagrams to the branching ratio for the decays being studied. We will do this by considering the example of the decay $B^- \rightarrow \mu^+ \mu^- \bar{\nu}_e e^-$. The contribution of the diagram in Fig. 1 can be estimated on the basis of the VMD model, taking into account only intermediate $\rho^0(770)$ - and $\omega(782)$ -meson states. By employing the values from [21], we then obtain

$$\begin{aligned} & \text{Br}^{(u)}(B^- \rightarrow \mu^+ \mu^- \bar{\nu}_e e^-) \\ & \approx \left| \sqrt{\text{Br}(B^- \rightarrow \rho^0 e^- \bar{\nu}_e) \text{Br}(\rho^0 \rightarrow \mu^+ \mu^-)} \right. \\ & \quad \left. + \sqrt{\text{Br}(B^- \rightarrow \omega e^- \bar{\nu}_e) \text{Br}(\omega \rightarrow \mu^+ \mu^-)} \right|^2 \\ & \approx 0.35 \times 10^{-7}. \end{aligned} \quad (7)$$

The amplitude corresponding to the diagrams in Fig. 2 is suppressed in relation to the amplitude for the diagram in Fig. 1 by the factor Λ/m_b , where m_b is the b -quark mass and $\Lambda \approx 300\text{--}500$ MeV. This follows from explicit expressions for the form factors for the leptonic rare radiative decays of B mesons [15, 22]. However, the contribution of the diagram in Fig. 2 to the total decay width may prove to be negligible because of the interference between the diagrams in Figs. 1 and 2 in the photon-pole region.

For the massless lepton helicity is a conserved quantum number, there is no bremsstrahlung in this approximation. For nonzero lepton masses, the bremsstrahlung contribution becomes significant only in the narrow region around the value of $q_{\min}^2 =$

$4m_\mu^2$. Therefore, the same argument as that for the contribution of the diagram in Fig. 2 is applicable to the diagram in Fig. 3.

The alternative estimate given below for the total branching ratio for the decay $B^- \rightarrow \mu^+ \mu^- \bar{\nu}_e e^-$ indicates indirectly that it is necessary to take into account the diagrams in Figs. 2 and 3 along with the diagram in Fig. 1. It is well known that the decay $B^- \rightarrow e^- \bar{\nu}_e$ is helicity-suppressed by the factor $(m_e/M_1)^2$. A simple theoretical estimation [23] yields the following value of the branching ratio for this decay:

$$\begin{aligned} & \text{Br}(B^- \rightarrow \bar{\nu}_e e^-) \\ & = \tau_{B^-} \frac{G_F^2 |V_{ub}|^2 f_{B_u}^2 M_1^3}{8\pi} \left(\frac{m_e}{M_1} \right)^2 \approx 10^{-11}. \end{aligned}$$

Photon emission from the B^- meson removes the aforementioned suppression. In order of magnitude, we therefore have

$$\begin{aligned} & \text{Br}(B^- \rightarrow \mu^+ \mu^- \bar{\nu}_e e^-) \\ & \approx \text{Br}(B^- \rightarrow \bar{\nu}_e e^-) \cdot \alpha_{\text{em}}^2 \cdot \left(\frac{m_b}{m_e} \right)^2 \\ & \approx 0.5 \times 10^{-7}. \end{aligned} \quad (8)$$

From the above estimates, it then follows that

$$\begin{aligned} & \text{Br}(B^- \rightarrow \mu^+ \mu^- \bar{\nu}_e e^-) = \kappa \text{Br}^{(u)}(B^- \rightarrow \mu^+ \mu^- \bar{\nu}_e e^-) \\ & \sim 1.5 \times \text{Br}^{(u)}(B^- \rightarrow \mu^+ \mu^- \bar{\nu}_e e^-). \end{aligned}$$

If the contribution of the diagram in Fig. 1 were absolutely dominant, then it would have been reasonable to expect for the coefficient in the above relation a value that is closer to unity than $\kappa \sim 1.5$.

An independent estimate of the coefficient κ can be obtained from the following experimental constraint on the branching ratio for the decay $B^- \rightarrow \gamma e^- \bar{\nu}_e$ [21]:

$$\begin{aligned} & \text{Br}(B^- \rightarrow \mu^+ \mu^- \bar{\nu}_e e^-) \approx \alpha_{\text{em}} \text{Br}(B^- \rightarrow \gamma e^- \bar{\nu}_e) \\ & \leq \frac{6.1 \times 10^{-6}}{137} \approx 0.44 \times 10^{-7}. \end{aligned} \quad (9)$$

In that case, we have $\kappa \sim 1.3$, which does not disprove either the conclusion that it is necessary to take into account the diagrams in Figs. 2 and 3. We note that the estimates in (8) and (9) determine only the order of magnitude of $\text{Br}(B^- \rightarrow \mu^+ \mu^- \bar{\nu}_e e^-)$.

At first glance, the branching ratio for the decay $B^- \rightarrow e^+ e^- \bar{\nu}_\mu \mu^-$ may receive a significant contribution from the processes $B^- \rightarrow (J/\psi \rightarrow e^+ e^-) (K^- \rightarrow \mu^- \bar{\nu}_\mu)$ and $B^- \rightarrow (J/\psi \rightarrow e^+ e^-) (\pi^- \rightarrow \mu^- \bar{\nu}_\mu)$, which we disregarded in estimating the branching ratio for the decay $B^- \rightarrow$

$\mu^+\mu^-\bar{\nu}_e e^-$. If, however, the values of $c\tau_{\pi^-} \approx 7.8$ m and $c\tau_{K^-} \approx 3.7$ m are taken into consideration, it can be stated that the primary vertex of the decay $B^- \rightarrow J/\psi K^- (\pi^-)$ and the secondary version of the decay $K^- (\pi^-) \rightarrow \mu^-\bar{\nu}_\mu$ are well resolved experimentally. Therefore, this cascade process can readily be distinguished experimentally from the decay $B^- \rightarrow e^+e^-\bar{\nu}_\mu\mu^-$.

Thus, the above estimates suggest that, for the $B^- \rightarrow \ell^+\ell^-\bar{\nu}_{\ell'}\ell'^-$ branching ratio, it is natural to expect a value around 10^{-7} . Of course, decays characterized by such a branching-ratio value are rare, but they are not extremely rare and therefore are quite observable, for example, at the LHCb setup of the LHC at CERN.

4. EXACT FORMULAS FOR $B^- \rightarrow \ell^+\ell^-\bar{\nu}_{\ell'}\ell'^-$ DECAYS

Let us consider the decay processes $B^- \rightarrow \mu^+\mu^-\bar{\nu}_e e^-$ and $B^- \rightarrow e^+e^-\bar{\nu}_\mu\mu^-$, in which negatively charged light leptons have different flavors in the final state. In a general form, these decays can be represented as $B^- \rightarrow \ell^+\ell^-\bar{\nu}_{\ell'}\ell'^-$ for $\ell \neq \ell'$.

The contribution of the diagram in Fig. 1 to the total amplitude for the $B^-(p) \rightarrow \ell^+(k_1)\ell^-(k_2)\bar{\nu}_{\ell'}(k_3)\ell'^-(k_4)$ decay can be calculated in the approximation of the VMD model (see Fig. 4). Upon setting $m_\ell = m_{\ell'} = 0$ and making use of the explicit expression (1) for the effective Hamiltonian, it can be found that within the VMD model, the contribution of the process depicted in Fig. 1 is described by the diagram in Fig. 4; that is,

$$\mathcal{M}_{fi}^{(u)} = \mathcal{A} \frac{1}{q^2} \times \left[\sum_{i=\rho^0, \omega} \frac{M_{2i}^2}{f_{V_i}} \frac{1}{q^2 - M_{2i}^2 + i\Gamma_{2i}M_{2i}} \mathcal{F}_{\mu\nu}^{(i)}(k^2) \right] \times j^\nu(k_2, k_1) J^\mu(k_4, k_3), \quad (10)$$

where, with allowance for the equations of motion, we have

$$\mathcal{F}_{\mu\nu}^{(i)}(k^2) = \frac{2V^{(i)}(k^2)}{M_1 + M_{2i}} \epsilon_{\mu\nu kq} - i(M_1 + M_{2i})A_1^{(i)}(k^2)g_{\mu\nu} + 2i\frac{A_2^{(i)}(k^2)}{M_1 + M_{2i}}q_\mu k_\nu.$$

We note that, in calculating the sum over resonances in expression (10), we take into account only the contributions of the lightest ρ^0 and ω mesons containing a $u\bar{u}$ pair.

The contribution of the process in Fig. 2 is described by the diagram in Fig. 5. This diagram is the

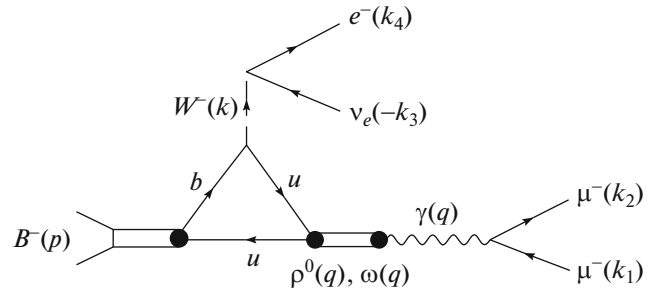


Fig. 4. Diagram for calculating $\mathcal{M}_{fi}^{(u)}$ [see Eq. (10)] for the decay $B^- \rightarrow \mu^+\mu^-\bar{\nu}_e e^-$. Virtual-photon emission from the light quark is described on the basis of the VMD model.

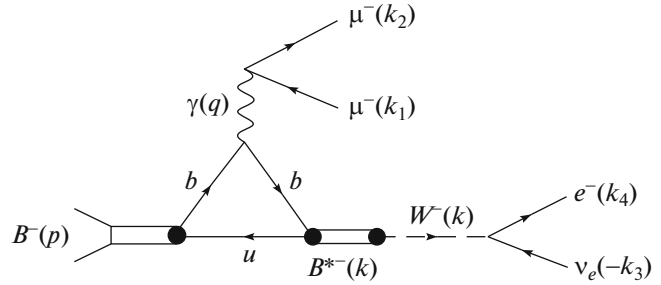


Fig. 5. Diagram for calculating $\mathcal{M}_{fi}^{(b)}$ [see Eq. (11)] for the decay $B^- \rightarrow \mu^+\mu^-\bar{\nu}_e e^-$.

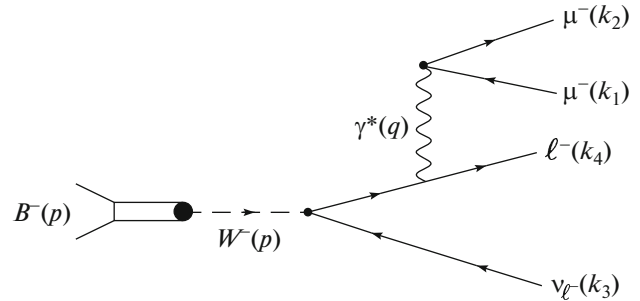


Fig. 6. Diagram for calculating the bremsstrahlung amplitude $\mathcal{M}_{fi}^{(\text{brem})}$ [see Eq. (12)] for the decay $B^- \rightarrow \mu^+\mu^-\bar{\nu}_e e^-$.

crossing channel of the $B^* \rightarrow B\gamma^*$ decay of a heavy vector meson to a heavy pseudoscalar meson and a virtual photon; that is,

$$\mathcal{M}_{fi}^{(b)} = \frac{2\mathcal{A}}{3} \frac{1}{q^2} \frac{M_{B^*} f_{B^*}}{k^2 - M_{B^*}^2 + i\Gamma_{B^*} M_{B^*}} \times \frac{V_b(q^2)}{M_1 + M_{B^*}} \epsilon_{\mu\nu kq} j^\nu(k_2, k_1) J^\mu(k_4, k_3). \quad (11)$$

Finally, the contribution corresponding to Fig. 3 and involving virtual-photon bremsstrahlung is described with the aid of the diagram in Fig. 6:

$$\mathcal{M}_{fi}^{(\text{brem})} = \mathcal{A} \frac{if_{B_u}}{q^2} g_{\mu\nu} j^\nu(k_2, k_1) J^\mu(k_4, k_3). \quad (12)$$

In expressions (10)–(12), we employed the following conventions:

$$\mathcal{A} = -\frac{G_F}{\sqrt{2}} 4\pi\alpha_{\text{em}} V_{ub},$$

$$j^\nu(k_2, k_1) = (\bar{\ell}(k_2)\gamma^\nu\ell(-k_1)),$$

$$\text{and } J^\mu(k_4, k_3) = (\bar{\ell}'(k_4)\gamma^\mu(1-\gamma^5)\nu_{\ell'}(-k_3)).$$

The total amplitude for the $B^-(p) \rightarrow \ell^+(k_1) \times \ell^-(k_2)\bar{\nu}_{\ell'}(k_3)\ell'^-(k_4)$ decay has the form

$$\begin{aligned} \mathcal{M}_{fi}^{(1234)} &= \mathcal{M}_{fi}^{(u)} + \mathcal{M}_{fi}^{(b)} + \mathcal{M}_{fi}^{(\text{brem})} \\ &= \frac{\mathcal{A}}{q^2} \left[\frac{a(q^2, k^2)}{M_1} \varepsilon_{\mu\nu kq} \right. \\ &\quad \left. - iM_1 b(q^2, k^2) g_{\mu\nu} + 2i \frac{c(q^2, k^2)}{M_1} q_\mu k_\nu \right] \\ &\quad \times j^\nu(k_2, k_1) J^\mu(k_4, k_3). \end{aligned} \quad (13)$$

The reason why it is convenient to choose the notation $\mathcal{M}_{fi}^{(1234)}$ for the total decay amplitude will become clear upon considering decays where final-state charged fermions are identical (see Section 5). The explicit expressions for the dimensionless functions $a(q^2, k^2) \equiv a(x_{12}, x_{34})$, $b(q^2, k^2) \equiv b(x_{12}, x_{34})$ and $c(q^2, k^2) \equiv c(x_{12}, x_{34})$ have the form

$$\begin{aligned} a(x_{12}, x_{34}) &= \frac{1}{3} \frac{\hat{M}_{B^*} \hat{f}_{B^*}}{x_{34} - \hat{M}_{B^*}^2 + i\hat{\Gamma}_{B^*} \hat{M}_{B^*}} \\ &\quad \times \frac{2V_b(M_1^2 x_{12})}{1 + \hat{M}_{B^*}} + \sum_{i=\rho^0, \omega} \frac{\hat{M}_{2i}^2}{f_{V_i}} \\ &\quad \times \frac{1}{x_{12} - \hat{M}_{2i}^2 + i\hat{\Gamma}_{2i} \hat{M}_{2i}} \frac{2V^{(i)}(M_1^2 x_{34})}{1 + \hat{M}_{2i}}, \\ b(x_{12}, x_{34}) &= -\hat{f}_{B_u} + \sum_{i=\rho^0, \omega} \frac{\hat{M}_{2i}^2}{f_{V_i}} \\ &\quad \times \frac{1}{x_{12} - \hat{M}_{2i}^2 + i\hat{\Gamma}_{2i} \hat{M}_{2i}} (1 + \hat{M}_{2i}) A_1^{(i)}(M_1^2 x_{34}); \\ c(x_{12}, x_{34}) &= \sum_{i=\rho^0, \omega} \frac{\hat{M}_{2i}^2}{f_{V_i}} \\ &\quad \times \frac{1}{x_{12} - \hat{M}_{2i}^2 + i\hat{\Gamma}_{2i} \hat{M}_{2i}} \frac{A_2^{(i)}(M_1^2 x_{34})}{1 + \hat{M}_{2i}}, \end{aligned} \quad (14)$$

where the dimensionless variables $x_{12} = q^2/M_1^2$ and $x_{34} = k^2/M_1^2$ are defined in the Appendix, while the dimensionless constants are given by $\hat{f}_{B_u} = f_{B_u}/M_1$, $\hat{f}_{B^*} = f_{B^*}/M_1$, $\hat{M}_{2i} = M_{2i}/M_1$, $\hat{M}_{B^*} = M_{B^*}/M_1$, $\hat{\Gamma}_{2i} = \Gamma_{2i}/M_1$, and $\hat{\Gamma}_{B^*} = \Gamma_{B^*}/M_1$. The form factors

$V_b(q^2)$, $V^{(i)}(k^2)$, $A_1^{(i)}(k^2)$, and $A_2^{(i)}(k^2)$ are also dimensionless functions.

The $B^- \rightarrow \ell^+ \ell^- \bar{\nu}_{\ell'} \ell'^-$ differential branching ratio can be calculated by the formula

$$\begin{aligned} d\text{Br}(B^- \rightarrow \ell^+ \ell^- \bar{\nu}_{\ell'} \ell'^-) \\ = \tau_{B^-} \frac{\sum_{s_1, s_2, s_3, s_4} |\mathcal{M}_{fi}^{(1234)}|^2}{2M_1} d\Phi_4^{(1234)}, \end{aligned} \quad (15)$$

where τ_{B^-} is the B^- -meson lifetime, the four-body phase space $d\Phi_4^{(1234)}$ is given by the expression (A.2), and summation is performed over the spins of final-state fermions. In expression (A.2), integration with respect to the angular variables y_{12} , y_{34} , and φ is removed analytically. As a result, we arrive at

$$\begin{aligned} \frac{d^2\text{Br}(B^- \rightarrow \ell^+ \ell^- \bar{\nu}_{\ell'} \ell'^-)}{dx_{12} dx_{34}} &= \tau_{B^-} \frac{G_F^2 M_1^5 \alpha_{\text{em}}^2 |V_{ub}|^2}{2^6 3^2 \pi^3} \\ &\quad \times \frac{\lambda^{1/2}(1, x_{12}, x_{34})}{x_{12}^2} \left[2x_{12} x_{34} \lambda(1, x_{12}, x_{34}) \right. \\ &\quad \times \left| a(x_{12}, x_{34}) \right|^2 + (\lambda(1, x_{12}, x_{34}) + 12x_{12} x_{34}) \\ &\quad \times \left| b(x_{12}, x_{34}) \right|^2 + \lambda^2(1, x_{12}, x_{34}) \left| c(x_{12}, x_{34}) \right|^2 \\ &\quad \left. + 2\lambda(1, x_{12}, x_{34})(x_{12} + x_{34} - 1) \right. \\ &\quad \left. \times \text{Re}(b(x_{12}, x_{34})c^*(x_{12}, x_{34})) \right], \end{aligned} \quad (16)$$

An ultimate integration of this expression with respect to x_{12} and x_{34} can be performed only numerically.

5. EXACT FORMULAS FOR THE $B^- \rightarrow \ell^+ \bar{\nu}_{\ell'} \ell^-$ DECAYS

At almost all of the experimental setups used, muon tracks are identified much better than signals from electrons. From the experimental point of view, the decay $B^- \rightarrow \mu^+ \bar{\nu}_\mu \mu^- \mu^-$ is therefore of greatest interest for detection. In this decay, the final state involves two identical negatively charged muons. This entails the need for taking into account Fermi's antisymmetry.

Let us consider $B^-(p) \rightarrow \ell^+(k_1) \bar{\nu}_{\ell'}(k_3) \ell^-(k_2) \ell^-(k_4)$ total decay amplitude. In the limit of zero lepton masses, the calculation described below is also applicable both to the decay $B^- \rightarrow \mu^+ \bar{\nu}_\mu \mu^- \mu^-$ and to the decay $B^- \rightarrow e^+ \bar{\nu}_e e^- e^-$. The total decay amplitude has the form

$$\mathcal{M}_{fi}^{(\text{tot})} = \mathcal{M}_{fi}^{(1234)} - \mathcal{M}_{fi}^{(1432)}, \quad (17)$$

where the amplitude $\mathcal{M}_{fi}^{(1234)}$ is given by expression (13), while the amplitude $\mathcal{M}_{fi}^{(1432)}$ is obtained

from $\mathcal{M}_{fi}^{(1234)}$ upon the substitution $k_2 \leftrightarrow k_4$. The consequence is that, in order to calculate $\mathcal{M}_{fi}^{(1432)}$, it is necessary to make the substitutions $q_\mu \rightarrow \tilde{q}_\mu, k_\mu \rightarrow$

$\tilde{k}_\mu, x_{12} \rightarrow x_{14}$, and $x_{34} \rightarrow x_{23}$ in Eqs. (13) and (14) (see Appendix).

The differential branching ratio is given by

$$d\text{Br}(B^- \rightarrow \ell^+ \bar{\nu}_\ell \ell^- \ell^-) = \frac{1}{2} \left[\tau_{B^-} \frac{\sum_{s_1, s_2, s_3, s_4} |\mathcal{M}_{fi}^{(1234)}|^2}{2M_1} d\Phi_4^{(1234)} + \tau_{B^-} \frac{\sum_{s_1, s_2, s_3, s_4} |\mathcal{M}_{fi}^{(1432)}|^2}{2M_1} d\Phi_4^{(1432)} - \tau_{B^-} \frac{\sum_{s_1, s_2, s_3, s_4} (\mathcal{M}_{fi}^{(1234)\dagger} \mathcal{M}_{fi}^{(1432)} + \mathcal{M}_{fi}^{(1432)\dagger} \mathcal{M}_{fi}^{(1234)})}{2M_1} d\Phi_4^{(1234)} \right], \quad (18)$$

where $d\Phi_4^{(1234)}$ and $d\Phi_4^{(1432)}$ are given by expressions (A.2) and (A.3), respectively. The common factor of 1/2 stems from Fermi's antisymmetry.

One can readily see that the first and second terms in expression (18) are equal to each other. For the respective branching ratio, we therefore have

$$\text{Br}(B^- \rightarrow \ell^+ \bar{\nu}_\ell \ell^- \ell^-) = \text{Br}(B^- \rightarrow \ell^+ \ell^- \bar{\nu}_\ell \ell^-) - \text{Br}_{\text{interf}}(B^- \rightarrow \ell^+ \bar{\nu}_\ell \ell^- \ell^-), \quad (19)$$

where

$$\begin{aligned} & \text{Br}_{\text{interf}}(B^- \rightarrow \ell^+ \bar{\nu}_\ell \ell^- \ell^-) \\ &= \frac{\tau_{B^-}}{4M_1} \int \sum_{s_1, s_2, s_3, s_4} (\mathcal{M}_{fi}^{(1234)\dagger} \mathcal{M}_{fi}^{(1432)} \\ &+ \mathcal{M}_{fi}^{(1432)\dagger} \mathcal{M}_{fi}^{(1234)}) d\Phi_4^{(1234)}. \end{aligned} \quad (20)$$

From Eq. (20), it follows that, in order to calculate the interference contribution, it is necessary to perform a five-dimensional numerical integrations. In doing this, it is necessary to make in the matrix element $\mathcal{M}_{fi}^{(1432)}$ the substitutions specified by Eqs. (A.4).

6. NUMERICAL RESULTS

In order to obtain branching ratios and to find the shapes of differential distributions, use is made of the numerical values of the masses, lifetimes, and decay widths for pseudoscalar and vector mesons and of the respective elements of the Kabibbo–Kabayashi–Maskawa matrix from [21]. In addition, the constants $f_{\rho(770)} = 5.04$ and $f_{\omega(782)} = 17.1$ were calculated in [24].

Convenient parametrizations of the hadron form factors (3) other than the electromagnetic form factor $V_b(q^2)$ were constructed in [20]. By employing general expressions from [25, 26], a parametrization of

the form factor $V_b(q^2)$ calculated within the dispersion formulation of the quark model can be obtained in the form [27]

$$V_b(q^2) = \frac{1.044}{\left(1 - \frac{q^2}{M_\Upsilon^2}\right) \left(1 - 0.81 \frac{q^2}{M_\Upsilon^2}\right)}, \quad (21)$$

where M_Υ is the $\Upsilon(1S)$ -meson mass. For the leptonic constants, the same method yields the values of $f_{B_u} = 191$ MeV and $f_{B^*} = 183$ MeV.

Let us consider the decay process $B^- \rightarrow \mu^+ \mu^- \bar{\nu}_e e^-$. As was discussed in Section 3, the value of $x_{12\text{min}} = q_{\text{min}}^2/M_1^2 = (2m_\mu/M_1)^2 \approx 0.0016$ provides a natural cutoff for the pole in x_{12} in calculating the branching ratio for this decay. The numerical integration of expression (16) with respect to x_{12} and x_{34} then yields

$$\begin{aligned} \text{Br}(B^- \rightarrow \mu^+ \mu^- \bar{\nu}_e e^-) &\approx 1.3 \frac{\tau_{B^-}}{1.638 \times 10^{-12} \text{ s}} \\ &\times \frac{|V_{ub}|^2}{1.67 \times 10^{-5}} \times 10^{-7}. \end{aligned} \quad (22)$$

An uncertainty in this result at a fixed value of q_{min}^2 in the range of $q_{\text{min}}^2 \leq 1 \text{ GeV}^2$ does not exceed 20% and depends largely on the uncertainty in the calculation of the hadron form factors for the $B \rightarrow \rho(770)$ and $B \rightarrow \omega(782)$ transitions [20]. We note that the numerical result in (22) is on the same order of magnitude as the estimates in (8) and (9) from Section 3, but it exceeds them numerically. This is because the estimations in Section 3 do not take fully into account the contribution of the pole in the variable q^2 . The importance of the pole contribution is obvious from the shape of the double-differential distribution $d^2\text{Br}(B^- \rightarrow \mu^+ \mu^- \bar{\nu}_e e^-)/dx_{12}dx_{34}$ in Fig. 7. The pole that arises in the limit of $x_{12} \rightarrow x_{12\text{min}} = q_{\text{min}}^2/M_1^2$ and whose contribution determines the maximum of the matrix element stands out in this figure along with the ridge of the narrow $\omega(782)$

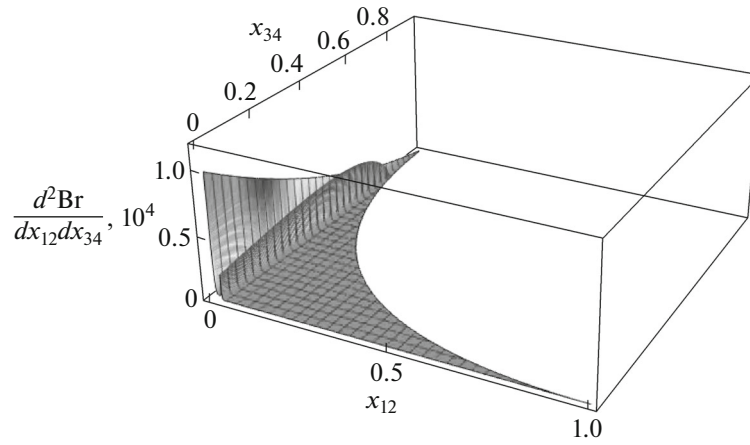


Fig. 7. Double-differential distribution $\frac{d^2 \text{Br}(B^- \rightarrow \mu^+ \mu^- \bar{\nu}_e e^-)}{dx_{12} dx_{34}}, 10^4$ calculated according to Eq. (16).

resonance. Because of the broad width, the $\rho^0(770)$ vector meson also makes a significant contribution to the respective branching ratio, but its manifestation in the distribution in Fig. 7 is less distinct.

Usually, the dimuon-detection efficiently is moderately low in the small- q^2 region. As a rule, it is therefore difficult to perform direct observations in the region of $\sqrt{q^2}$ around a few hundred MeV units and below. In view of this, the $\sqrt{q_{\min}^2}$ dependence of $\text{Br}(B^- \rightarrow \mu^+ \mu^- \bar{\nu}_e e^-)$ is of interest for performing a correct comparison of the theory and experiment. This dependence is illustrated in Fig. 8. In order to the render the use of these results convenient, they are also presented in the table. From Fig. 8 and

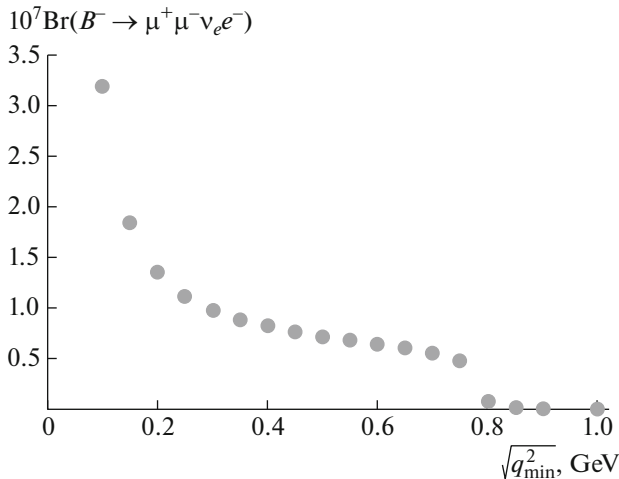


Fig. 8. Branching ratio $\text{Br}(B^- \rightarrow \mu^+ \mu^- \bar{\nu}_e e^-)$ as a function of $\sqrt{q_{\min}^2}$, which is the threshold for integration with respect to the variable q^2 [or x_{12} in expression (16)]. The points on the graph correspond to the data in the table.

from the table, one can see that, according to the model used, the $B^- \rightarrow \mu^+ \mu^- \bar{\nu}_e e^-$ branching ratio is negligible in the region of $x_{12} > (M_{\omega(782)}/M_1)^2$ since it is determined by the tails of the $\rho^0(770)$ and $\omega(782)$ resonances. Therefore, it seems that the approximation considered here, in which one takes into account only the contribution of the lightest resonances, $\rho(770)$ and $\omega(782)$, becomes inapplicable in the case of measurements of the $B^- \rightarrow \mu^+ \mu^- \bar{\nu}_e e^-$ branching ratio in the region of $q^2 > 1 \text{ GeV}^2$, where it would be desirable to take into account the $\omega(1420)$, $\rho(1450)$, $\omega(1650)$, and $\rho(1700)$ contributions. We note that the inclusion of four heavy resonances would have virtually no effect on the result in (22) but would determine the behavior of the branching ratio in the region of $q^2 > 1 \text{ GeV}^2$. Let us now consider the decay process $B^- \rightarrow e^+ e^- \bar{\nu}_\mu \mu^-$. A formal integration in the region of the photon pole with respect to the variable q^2 (or the variable x_{12}) leads to the dependence

$$\text{Br} \sim \int \frac{dx_{12}}{x_{12}^2} \sim \frac{1}{x_{12\min}}.$$

In order of magnitude, we therefore have

$$\begin{aligned} & \text{Br}(B^- \rightarrow e^+ e^- \bar{\nu}_\mu \mu^-) \\ & \sim \left(\frac{\sqrt{q_{\min}^2}}{2m_e} \right)^2 \text{Br}(B^- \rightarrow \mu^+ \mu^- \bar{\nu}_e e^-). \end{aligned}$$

From the experimental point of view, however, such a prediction is meaningless since the region around $x_{12} \sim (2m_e/M_1)^2 \approx 3.7 \times 10^{-8}$ is inaccessible to direct measurements. As was indicated above, the region of measurements in the variable q^2 starts from about 100 MeV. Physically, only the following statement is therefore meaningful: at a fixed value of $\sqrt{q_{\min}^2}$

Branching ratio $\text{Br}(B^- \rightarrow \mu^+ \mu^- \bar{\nu}_e e^-)$ versus $\sqrt{q_{\min}^2}$, which is the threshold for integration with respect to the variable q^2 [or x_{12} in expression (16)] (the data in the table correspond to the points in Fig. 8)

$\sqrt{q_{\min}^2}$, GeV	$\text{Br}(B^- \rightarrow \mu^+ \mu^- \bar{\nu}_e e^-)$
0.10	$3.2 \frac{\tau_{B^-}}{1.638 \times 10^{-12} \text{ s}} \frac{ V_{ub} ^2}{1.67 \times 10^{-5}} \times 10^{-7}$
0.15	$1.8 \frac{\tau_{B^-}}{1.638 \times 10^{-12} \text{ s}} \frac{ V_{ub} ^2}{1.67 \times 10^{-5}} \times 10^{-7}$
0.20	$1.4 \frac{\tau_{B^-}}{1.638 \times 10^{-12} \text{ s}} \frac{ V_{ub} ^2}{1.67 \times 10^{-5}} \times 10^{-7}$
0.25	$1.1 \frac{\tau_{B^-}}{1.638 \times 10^{-12} \text{ s}} \frac{ V_{ub} ^2}{1.67 \times 10^{-5}} \times 10^{-7}$
0.30	$9.8 \frac{\tau_{B^-}}{1.638 \times 10^{-12} \text{ s}} \frac{ V_{ub} ^2}{1.67 \times 10^{-5}} \times 10^{-8}$
0.35	$8.9 \frac{\tau_{B^-}}{1.638 \times 10^{-12} \text{ s}} \frac{ V_{ub} ^2}{1.67 \times 10^{-5}} \times 10^{-8}$
0.40	$8.2 \frac{\tau_{B^-}}{1.638 \times 10^{-12} \text{ s}} \frac{ V_{ub} ^2}{1.67 \times 10^{-5}} \times 10^{-8}$
0.45	$7.7 \frac{\tau_{B^-}}{1.638 \times 10^{-12} \text{ s}} \frac{ V_{ub} ^2}{1.67 \times 10^{-5}} \times 10^{-8}$
0.50	$7.2 \frac{\tau_{B^-}}{1.638 \times 10^{-12} \text{ s}} \frac{ V_{ub} ^2}{1.67 \times 10^{-5}} \times 10^{-8}$
0.55	$6.8 \frac{\tau_{B^-}}{1.638 \times 10^{-12} \text{ s}} \frac{ V_{ub} ^2}{1.67 \times 10^{-5}} \times 10^{-8}$
0.60	$6.5 \frac{\tau_{B^-}}{1.638 \times 10^{-12} \text{ s}} \frac{ V_{ub} ^2}{1.67 \times 10^{-5}} \times 10^{-8}$
0.65	$6.0 \frac{\tau_{B^-}}{1.638 \times 10^{-12} \text{ s}} \frac{ V_{ub} ^2}{1.67 \times 10^{-5}} \times 10^{-8}$
0.70	$5.5 \frac{\tau_{B^-}}{1.638 \times 10^{-12} \text{ s}} \frac{ V_{ub} ^2}{1.67 \times 10^{-5}} \times 10^{-8}$
0.75	$4.8 \frac{\tau_{B^-}}{1.638 \times 10^{-12} \text{ s}} \frac{ V_{ub} ^2}{1.67 \times 10^{-5}} \times 10^{-8}$
0.80	$7.1 \frac{\tau_{B^-}}{1.638 \times 10^{-12} \text{ s}} \frac{ V_{ub} ^2}{1.67 \times 10^{-5}} \times 10^{-9}$
0.85	$2.2 \frac{\tau_{B^-}}{1.638 \times 10^{-12} \text{ s}} \frac{ V_{ub} ^2}{1.67 \times 10^{-5}} \times 10^{-9}$
0.90	$9.0 \frac{\tau_{B^-}}{1.638 \times 10^{-12} \text{ s}} \frac{ V_{ub} ^2}{1.67 \times 10^{-5}} \times 10^{-10}$
1.00	$3.0 \frac{\tau_{B^-}}{1.638 \times 10^{-12} \text{ s}} \frac{ V_{ub} ^2}{1.67 \times 10^{-5}} \times 10^{-10}$

in the region of $\sqrt{q_{\min}^2} > 2m_\mu$, the relation

$$\frac{\text{Br}(B^- \rightarrow \mu^+ \mu^- \bar{\nu}_e e^-)}{\text{Br}(B^- \rightarrow e^+ e^- \bar{\nu}_\mu \mu^-)} \bigg|_{\sqrt{q_{\min}^2} > 2m_\mu} = 1 \quad (23)$$

should hold by virtue of lepton universality. Equation (23) may prove to be of use as an independent test of lepton universality in rare decays of B mesons, since, at the present time, there are indications of a lepton-universality violation in such decays (in this

connection, see, for example, the discussion on the lepton-universality problem in [28, 29]).

Let us consider predictions for the decay process $B^- \rightarrow \mu^+ \bar{\nu}_\mu \mu^- \mu^-$. For the interference contribution, a numerical integration of expression (20) at $x_{12\min} = (2m_\mu/M_1)^2$ yields the value

$$\text{Br}_{\text{interf}}(B^- \rightarrow \mu^+ \bar{\nu}_\mu \mu^- \mu^-) \approx -2.1 \times 10^{-9},$$

which is one order of magnitude smaller than the uncertainty associated with nonperturbative strong-interaction effects contributing to the branching ratio for the decay being considered. Thus, we can state that, in the limit of zero lepton masses, it follows from the results presented in (19) and (22) that, to a precision of 20%, there arises the relation

$$\begin{aligned} \text{Br}(B^- \rightarrow \mu^+ \bar{\nu}_\mu \mu^- \mu^-) &\approx 1.3 \frac{\tau_{B^-}}{1.638 \times 10^{-12} \text{ s}} \\ &\times \frac{|V_{ub}|^2}{1.67 \times 10^{-5}} \times 10^{-7}, \end{aligned} \quad (24)$$

which we obtained at $x_{12\min} = (2m_\mu/M_1)^2$.

The same arguments as those used in evaluating the pole contribution from a virtual photon in the decay $B^- \rightarrow e^+ e^- \bar{\nu}_\mu \mu^-$ apply to integration around to photon pole in the decay $B^- \rightarrow e^+ \bar{\nu}_e e^- e^-$. By employing lepton universality, we therefore obtain

$$\frac{\text{Br}(B^- \rightarrow \mu^+ \bar{\nu}_\mu \mu^- \mu^-)}{\text{Br}(B^- \rightarrow e^+ \bar{\nu}_e e^- e^-)} \bigg|_{\sqrt{q_{\min}^2} > 2m_\mu, \sqrt{q_{\min}^2} > 2m_\mu} = 1. \quad (25)$$

7. ESTIMATION OF BRANCHING RATIOS FOR $B_{d,s} \rightarrow \ell^+ \ell^- \ell'^+ \ell'^-$ AND $B_{d,s} \rightarrow \ell^+ \ell^- \ell^+ \ell^-$ DECAYS

By employing the numerical results in (22) and (24), we can estimate $\text{Br}(B_{s,d} \rightarrow \mu^+ \mu^- e^+ e^-)$ and $\text{Br}(B_{s,d} \rightarrow \mu^+ \mu^- \mu^+ \mu^-)$. Such estimations are of great topical interest, since upper limits on $\text{Br}(B_{d,s} \rightarrow \mu^+ \mu^- \mu^+ \mu^-)$ have already been obtained at the LHCb setup [18, 19]. In the only study where the branching-ratio values were predicted for the decays $B_s \rightarrow \mu^+ \mu^- \mu^+ \mu^-$ and $B_s \rightarrow e^+ e^- \mu^+ \mu^-$ and which was reported in [30], the contributions of intermediate vector resonances and weak annihilation were disregarded. There are no predictions for $\text{Br}(B_d \rightarrow \mu^+ \mu^- \mu^+ \mu^-)$ and $\text{Br}(B_d \rightarrow e^+ e^- \mu^+ \mu^-)$ in the literature.

If one assumes that the nonperturbative strong-interaction contributions to the $B^- \rightarrow \ell^+ \ell^- \nu_{\ell'} \ell'^-$ and $B_{d,s} \rightarrow \ell^+ \ell^- \ell'^+ \ell'^-$ total decay amplitudes are on the same order of magnitude, then the respective branching ratios differ only because of electroweak

factors by which the hadron amplitudes are multiplied. We then have the following estimates:

$$\begin{aligned} \text{Br}(B_s \rightarrow \mu^+ \mu^- e^+ e^-) &\sim \frac{\tau_{B_s}}{\tau_{B^-}} \frac{\alpha_{\text{em}}^2}{8\pi^2} |C_{10A}|^2 \frac{|V_{tb} V_{ts}^*|^2}{|V_{ub}|^2} \\ &\times \left(\frac{M_{B_s}}{M_{B^-}} \right)^5 \text{Br}(B^- \rightarrow e^+ e^- \bar{\nu}_\mu \mu^-) \\ &\approx 1.8 \times 10^{-10}, \end{aligned} \quad (26)$$

where $|C_{10A}| = 4.64$ is the Wilson coefficient in the effective Hamiltonian for the $b \rightarrow (d, s)\ell^+\ell^-$ [5] transitions, and

$$\begin{aligned} &\text{Br}(B_d \rightarrow \mu^+ \mu^- e^+ e^-) \\ &\approx \frac{\tau_{B_d}}{\tau_{B_s}} \frac{|V_{td}|^2}{|V_{ts}|^2} \left(\frac{M_{B_d}}{M_{B_s}} \right)^5 \text{Br}(B_s \rightarrow \mu^+ \mu^- e^+ e^-) \\ &\approx 8 \times 10^{-12}. \end{aligned} \quad (27)$$

The estimate in (26) differs from the analogous prediction in [30] by a factor smaller than two. In view of the roughness of the approximation used, this agreement should be thought to be fairly good. There are no predictions for B_d -meson decays in [30].

By analogy with expression (26) for $\text{Br}(B_s \rightarrow \mu^+ \mu^- \mu^+ \mu^-)$, we have

$$\begin{aligned} \text{Br}(B_s \rightarrow \mu^+ \mu^- \mu^+ \mu^-) &\sim \frac{1}{2} \frac{\tau_{B_s}}{\tau_{B^-}} \frac{\alpha_{\text{em}}^2}{8\pi^2} |C_{10A}|^2 \\ &\times \frac{|V_{tb} V_{ts}^*|^2}{|V_{ub}|^2} \left(\frac{M_{B_s}}{M_{B^-}} \right)^5 \text{Br}(B^- \rightarrow \mu^+ \bar{\nu}_\mu \mu^- \mu^-) \\ &\approx 0.9 \times 10^{-10}, \end{aligned} \quad (28)$$

where the additional factor of $1/2$ arises because of the second pair of identical fermions. The prediction in Eq. (28) is approximately 2.5 times as large as the respective result in [30].

The predictions of Dincer and Sehgal in [30] fall short of the estimates in Eqs. (26) and (28) since those authors took into consideration only electroweak contributions, disregarding hadron resonances.

The following relation is an analog of Eq. (27):

$$\begin{aligned} &\text{Br}(B_d \rightarrow \mu^+ \mu^- \mu^+ \mu^-) \\ &\approx \frac{\tau_{B_d}}{\tau_{B_s}} \frac{|V_{td}|^2}{|V_{ts}|^2} \left(\frac{M_{B_d}}{M_{B_s}} \right)^5 \text{Br}(B_s \rightarrow \mu^+ \mu^- \mu^+ \mu^-) \\ &\approx 4 \times 10^{-12}. \end{aligned} \quad (29)$$

Yet another independent estimate of the branching ratios for the four-leptonic rare decays $B_{d,s} \rightarrow \mu^+ \mu^- e^+ e^-$ and $B_{d,s} \rightarrow \mu^+ \mu^- \mu^+ \mu^-$ can be obtained by employing the numerical values of the branching ratios for the leptonic radiative rare decays $B_{d,s} \rightarrow$

$\mu^+ \mu^- \gamma$ and $B_{d,s} \rightarrow e^+ e^- \gamma$ from [22]. The proposed estimate would be similar to the estimate in Eq. (9).

In order to obtain an independent estimate, it is necessary to choose in Table III from [22] the values of the $B_{d,s} \rightarrow \ell^+ \ell^- \gamma$ branching ratios at $E_{\text{min}}^\gamma = 80$ MeV. This is a good approximation since the E_{min}^γ dependence of the $B_{d,s} \rightarrow \ell^+ \ell^- \gamma$ branching ratios is rather weak in the region of $E_{\text{min}}^\gamma \geq 80$ MeV. We emphasize that the $B_s \rightarrow \ell^+ \ell^- \gamma$ branching ratios from [22] should be multiplied by the factor 0.7. This factor reflects the difference in the numerical values of the elements of the Cabibbo–Kobayashi–Maskawa matrix between [22] and the present article. For $B_d \rightarrow \ell^+ \ell^- \gamma$ decays, this difference is insignificant.

Considering that the decays $B_{d,s} \rightarrow \mu^+ \mu^- e^+ e^-$ receive contributions from two processes, $B_{d,s} \rightarrow \mu^+ \mu^- \gamma^* \rightarrow \mu^+ \mu^- e^+ e^-$ and $B_{d,s} \rightarrow \gamma^* e^+ e^- \rightarrow \mu^+ \mu^- e^+ e^-$, we can obtain the following estimates for the branching ratios in question:

$$\begin{aligned} &\text{Br}(B_s \rightarrow \mu^+ \mu^- e^+ e^-) \\ &\sim \alpha_{\text{em}} (\text{Br}(B_s \rightarrow \mu^+ \mu^- \gamma) + \text{Br}(B_s \rightarrow e^+ e^- \gamma)) \\ &\approx 2.2 \times 10^{-10} \end{aligned} \quad (30)$$

and

$$\begin{aligned} &\text{Br}(B_d \rightarrow \mu^+ \mu^- e^+ e^-) \\ &\sim \alpha_{\text{em}} (\text{Br}(B_d \rightarrow \mu^+ \mu^- \gamma) + \text{Br}(B_d \rightarrow e^+ e^- \gamma)) \\ &\approx 3.8 \times 10^{-12}. \end{aligned} \quad (31)$$

The estimates in (26) and (30) for $\text{Br}(B_s \rightarrow \mu^+ \mu^- e^+ e^-)$ agree well with each other, whereas the estimates in (27) and (31) differ by a factor greater than two. However, this distinction is acceptable in estimations.

Finally, we will estimate $\text{Br}(B_{d,s} \rightarrow \mu^+ \mu^- \mu^+ \mu^-)$. By analogy with Eqs. (7) and (30), we have

$$\begin{aligned} &\text{Br}(B_s \rightarrow \mu^+ \mu^- \mu^+ \mu^-) \sim \frac{\alpha_{\text{em}}}{4} \\ &\times \left| \sqrt{\text{Br}(B_s \rightarrow \mu^+ \mu^- \gamma)} + \sqrt{\text{Br}(B_s \rightarrow \mu^+ \mu^- \gamma)} \right|^2 \\ &\approx 1.0 \times 10^{-10}; \\ &\text{Br}(B_d \rightarrow \mu^+ \mu^- \mu^+ \mu^-) \sim \frac{\alpha_{\text{em}}}{4} \\ &\times \left| \sqrt{\text{Br}(B_d \rightarrow \mu^+ \mu^- \gamma)} + \sqrt{\text{Br}(B_d \rightarrow \mu^+ \mu^- \gamma)} \right|^2 \\ &\approx 0.4 \times 10^{-12}. \end{aligned} \quad (32)$$

where $1/4$ is a statistical factor that corresponds to the permutations of identical fermions in two dimuons. In deriving the estimates in (32), we have considered that the reactions in question may proceed

in two ways: $B_{d,s} \rightarrow \mu^+ \mu^- \gamma^* \rightarrow \mu^+ \mu^- (\mu^+ \mu^-)$ and $B_{d,s} \rightarrow \gamma^* \mu^+ \mu^- \rightarrow (\mu^+ \mu^-) \mu^+ \mu^-$. A comparison of the numerical values in (28) and (29) with (32) is indicative of the need for directly calculating $\text{Br}(B_d \rightarrow \mu^+ \mu^- \mu^+ \mu^-)$, since various indirect estimations lead to results commensurate only in order of magnitude. At the same time, numerical agreement for $\text{Br}(B_s \rightarrow \mu^+ \mu^- \mu^+ \mu^-)$ is within an error of 10%.

8. CONCLUSIONS

The results of the present study can be summarized as follows.

(i) We have obtained a prediction for the $B^- \rightarrow \mu^+ \mu^- \bar{\nu}_e e^-$ branching ratios at a level of 1.3×10^{-7} at $\sqrt{q_{\min}^2} = 2m_\mu \approx 210$ MeV. This demonstrates the possibility of detecting the decay $B^- \rightarrow \mu^+ \mu^- \bar{\nu}_e e^-$ at the LHC (CERN) and at the Belle-II setup in Japan.

(ii) We have found the $\sqrt{q_{\min}^2}$ dependence of $\text{Br}(B^- \rightarrow \mu^+ \mu^- \bar{\nu}_e e^-)$. This dependence is given in Fig. 8 and in Table 1.

(iii) We have obtained numerical predictions for the $B^- \rightarrow \mu^+ \bar{\nu}_\mu \mu^- \mu^-$ branching ratio at $\sqrt{q_{\min}^2} = 2m_\mu \approx 210$ MeV with allowance for the Fermi interference contribution:

$$\text{Br}(B^- \rightarrow \mu^+ \bar{\nu}_\mu \mu^- \mu^-) \approx 1.3 \times 10^{-7}.$$

(iv) Tests of lepton universality in B^- -meson decays to three charged leptons and a neutrino have been proposed.

(v) The branching ratios for $B_{d,s}$ -meson decays to four charged leptons have been estimated as

$$\text{Br}(B_s \rightarrow \mu^+ \mu^- e^+ e^-) = (1.8-2.2) \times 10^{-10},$$

$$\text{Br}(B_s \rightarrow \mu^+ \mu^- \mu^+ \mu^-) = (0.9-1.0) \times 10^{-10},$$

$$\text{Br}(B_d \rightarrow \mu^+ \mu^- e^+ e^-) = (3.8-8.0) \times 10^{-12},$$

$$\text{Br}(B_d \rightarrow \mu^+ \mu^- \mu^+ \mu^-) = (0.4-4.0) \times 10^{-12}.$$

These estimates are in good agreement with the current experimental limits from [18, 19].

ACKNOWLEDGMENTS

We are grateful to I.M. Belyaev [Institute for Theoretical and Experimental Physics (ITEP), Moscow], E.E. Boos [Institute of Nuclear Physics at Moscow State University (INS MSU)], L.V. Dudko (INS MSU), V.Yu. Egorychev (ITEP), A.D. Kozachuk (INS MSU), and K.S. Toms (CERN) for stimulating discussions that contributed to the improvement of this research. Special thanks are due to D.I. Melikhov

for a discussion on the structure of hadron contributions to the amplitude for four-leptonic decays and for the derivation of Eq. (21).

This work was supported by the Russian Science Foundation within the project (no. 16-12-10280) Phenomenological Manifestations of Standard Model Extensions in Processes Involving the Top Quark.

Appendix

KINEMATICS OF FOUR-LEPTONIC DECAYS

We denote by k_i , $i = \{1, 2, 3, 4\}$, the 4-momenta of final-state leptons in the four-leptonic decays of B mesons. In the present study, $k_i^2 = 0$ for all i ; that is, we assume that these leptons are massless. We introduce the 4-momenta

$$q = k_1 + k_2; \quad k = k_3 + k_4; \quad \tilde{q} = k_1 + k_4;$$

$$\tilde{k} = k_2 + k_3; \quad p = k_1 + k_2 + k_3 + k_4,$$

where p is the B -meson 4-momentum and $p^2 = M_1^2$. For the ensuing calculations, it is convenient to employ the dimensionless variables

$$x_{12} = \frac{q^2}{M_1^2}, \quad x_{34} = \frac{k^2}{M_1^2},$$

$$x_{14} = \frac{\tilde{q}^2}{M_1^2}, \quad x_{23} = \frac{\tilde{k}^2}{M_1^2}.$$

The general notation for them is $x_{ij} = (k_i + k_j)^2 / M_1^2$. The ensuing calculations does not involve all of x_{ij} but only those of them that we presented above. We define the ranges of x_{ij} . With the aid of the inequality $(p_1 p_2) \geq \sqrt{p_1^2} \sqrt{p_2^2}$, we find for x_{12} that

$$0 \leq \frac{2(k_1 k_2)}{M_1^2} = \frac{(k_1 + k_2)^2}{M_1^2} = x_{12}.$$

Similarly, we can show that any x_{ij} is nonnegative. On the other hand, we have

$$\begin{aligned} 1 &= \frac{p^2}{M_1^2} = \frac{(q+k)^2}{M_1^2} = \frac{q^2 + k^2 + 2(qk)}{M_1^2} \\ &\geq \frac{q^2 + k^2 + 2\sqrt{q^2}\sqrt{k^2}}{M_1^2} = \frac{(\sqrt{q^2} + \sqrt{k^2})^2}{M_1^2} \\ &= (\sqrt{x_{12}} + \sqrt{x_{34}})^2. \end{aligned}$$

Since $0 \leq x_{34}$, we have $x_{12} \leq 1$. It follows that $x_{12} \in [0, 1]$. The upper boundary of the variable x_{34} depends on x_{12} . We have

$$x_{34} = \frac{(p-q)^2}{M_1^2} = \frac{M_1^2 + q^2 - 2(pq)}{M_1^2}$$

$$\leq \frac{M_1^2 + q^2 - 2M_1\sqrt{q^2}}{M_1^2} = \frac{(M_1 - \sqrt{q^2})^2}{M_1^2} \\ = (1 - \sqrt{x_{12}})^2.$$

It follows that, at a fixed value of the variable x_{12} , $x_{34} \in [0, (1 - \sqrt{x_{12}})^2]$.

Similar relations hold for the pair of x_{14} and x_{23} : $x_{14} \in [0, 1]$ and $x_{23} \in [0, (1 - \sqrt{x_{14}})^2]$ at a fixed value of x_{14} .

Let us consider the kinematics of $B^-(p) \rightarrow \ell^+(k_1)\ell^-(k_2)\bar{\nu}_{\ell'}(k_3)\ell'^-(k_4)$ decays for the case where the flavor of the negatively charged lepton $\ell^-(k_2)$ differs from the flavor of the negatively charged lepton $\ell'^-(k_4)$. We now assign the positively charged lepton the momentum \mathbf{k}_1 and the antineutrino the momentum \mathbf{k}_3 . This makes it possible to introduce the angle θ_{12} between the momentum of the positively charged lepton and the direction of B -meson motion (z axis) in the rest frame of the $\ell^+\ell^-$ pair and the angle

θ_{34} between the direction of antineutrino motion and the direction of B -meson motion (z axis) in the rest frame of the $\ell'^-\bar{\nu}_{\ell'}$ pair. We then have

$$y_{12} \equiv \cos \theta_{12} \\ = -\frac{2}{\lambda^{1/2}(1, x_{12}, x_{34})} (x_{13} + x_{14} - x_{23} - x_{24}), \\ y_{34} \equiv \cos \theta_{34} \\ = -\frac{2}{\lambda^{1/2}(1, x_{12}, x_{34})} (x_{13} + x_{23} - x_{14} - x_{24}),$$

where $\lambda(a, b, c) = a^2 + b^2 + c^2 - 2ab - 2ac - 2bc$ is the standard triangle function. The respective angles lie in the ranges of $\theta_{12} \in [0, \pi]$ and $\theta_{34} \in [0, \pi]$. Therefore, we have $y_{12} \in [-1, 1]$ and $y_{34} \in [-1, 1]$. The angles are measured from the z axis. In addition, it is necessary to determine the angle φ between the planes spanned by the $(\mathbf{k}_1, \mathbf{k}_2)$ and $(\mathbf{k}_3, \mathbf{k}_4)$ pairs of vectors. By employing the technique developed in [31], one can obtain an expression for $\cos \varphi$ in the form

$$\cos \varphi = \frac{\det \begin{pmatrix} M_1^2 & (pk_1) & (pk_2) \\ (pk_4) & (k_1k_4) & (k_2k_4) \\ (pk_3) & (k_1k_3) & (k_2k_3) \end{pmatrix}}{\sqrt{\det \begin{pmatrix} M_1^2 & (pk_1) & (pk_2) \\ (pk_1) & 0 & (k_1k_2) \\ (pk_2) & (k_1k_2) & 0 \end{pmatrix} \det \begin{pmatrix} M_1^2 & (pk_3) & (pk_4) \\ (pk_3) & 0 & (k_3k_4) \\ (pk_4) & (k_3k_4) & 0 \end{pmatrix}}}. \quad (\text{A.1})$$

The angle φ lies in the half-open interval of $\varphi \in [0, 2\pi]$. It is reckoned from the $(\mathbf{k}_1, \mathbf{k}_2)$ plane toward the $(\mathbf{k}_3, \mathbf{k}_4)$ plane.

The four-body phase space has the form

$$d\Phi_4^{(1234)} = M_1^4 \frac{dx_{12}}{2\pi} \frac{dx_{34}}{2\pi} d\Phi_2^{(qk)} d\Phi_2^{(12)} d\Phi_2^{(34)},$$

where

$$d\Phi_2^{(qk)} = 2\pi\delta(q^2 - x_{12}M_1^2) \\ \times \frac{d^4q}{(2\pi)^4} 2\pi\delta(k^2 - x_{34}M_1^2) \\ \times \frac{d^4k}{(2\pi)^4} (2\pi)^4 \delta^4(p - q - k), \\ d\Phi_2^{(12)} = 2\pi\delta(k_1^2) \frac{d^4k_1}{(2\pi)^4} 2\pi\delta(k_2^2)$$

$$\times \frac{d^4k_2}{(2\pi)^4} (2\pi)^4 \delta^4(q - k_1 - k_2),$$

$$d\Phi_2^{(34)} = 2\pi\delta(k_3^2) \frac{d^4k_3}{(2\pi)^4} 2\pi\delta(k_4^2) \\ \times \frac{d^4k_4}{(2\pi)^4} (2\pi)^4 \delta^4(k - k_3 - k_4)$$

In calculating the four-body phase space, it is convenient to choose x_{12} , x_{34} , y_{12} , y_{34} , and φ for independent variables of integration. We therefore have

$$\Phi_2^{(qk)} = \frac{1}{2^3\pi} \lambda^{1/2}(1, x_{12}, x_{34}); \\ d\Phi_2^{(12)} = \frac{1}{2^4\pi} dy_{12}; \quad d\Phi_2^{(34)} = \frac{1}{2^5\pi^2} dy_{34} d\varphi,$$

which yields

$$d\Phi_4^{(1234)} = \frac{M_1^4}{2^{14}\pi^6} \lambda^{1/2}(1, x_{12}, x_{34}) \times dx_{12} dx_{34} dy_{12} dy_{34} d\varphi. \quad (\text{A.2})$$

In the case of $B^-(p) \rightarrow \ell^+(k_1)\ell^-(k_2) \times \bar{\nu}_\ell(k_3)\ell^-(k_4)$ decays, there are two identical leptons in the final state, $\ell^-(k_2)$ and $\ell^-(k_4)$. Therefore, it is necessary to perform Fermi's antisymmetrization of the decay amplitude in the 4-momenta k_2 and k_4 . In calculating the respective branching ratio, we will need, in this case, an additional relation for the phase space in the form

$$d\Phi_4^{(1432)} = \frac{M_1^4}{2^{14}\pi^6} \lambda^{1/2}(1, x_{14}, x_{23}) \times dx_{14} dx_{23} dy_{14} dy_{23} d\tilde{\varphi}, \quad (\text{A.3})$$

where $\tilde{\varphi}$ is the angle between the $(\mathbf{k}_1, \mathbf{k}_4)$ and $(\mathbf{k}_2, \mathbf{k}_3)$ planes, which is reckoned from the $(\mathbf{k}_1, \mathbf{k}_4)$ plane. Expression (A.3) proves to be perfectly analogous to expression (A.2). As to $\cos \tilde{\varphi}$, we can find it by making the substitution $k_2 \leftrightarrow k_4$ in Eq. (A.1). In order to perform the required numerical integration, it is also necessary to express the variables x_{ij} in terms of $x_{12}, x_{34}, y_{12}, y_{34}$, and φ as

$$\begin{aligned} x_{13} &= \frac{1}{4} \left(-2\sqrt{x_{12}x_{34}(1-y_{12}^2)(1-y_{34}^2)} \right. \\ &\quad \times \cos \varphi + (1-x_{12}-x_{34})y_{12}y_{34} \\ &\quad \left. - \lambda^{1/2}(1, x_{14}, x_{23})(y_{12}+y_{34}) + 1-x_{12}-x_{34} \right); \\ x_{14} &= \frac{1}{4} \left(2\sqrt{x_{12}x_{34}(1-y_{12}^2)(1-y_{34}^2)} \right. \\ &\quad \times \cos \varphi - (1-x_{12}-x_{34})y_{12}y_{34} \\ &\quad \left. - \lambda^{1/2}(1, x_{14}, x_{23})(y_{12}-y_{34}) + 1-x_{12}-x_{34} \right); \\ x_{23} &= \frac{1}{4} \left(2\sqrt{x_{12}x_{34}(1-y_{12}^2)(1-y_{34}^2)} \right. \\ &\quad \times \cos \varphi - (1-x_{12}-x_{34})y_{12}y_{34} \\ &\quad \left. + \lambda^{1/2}(1, x_{14}, x_{23})(y_{12}-y_{34}) + 1-x_{12}-x_{34} \right); \\ x_{24} &= \frac{1}{4} \left(-2\sqrt{x_{12}x_{34}(1-y_{12}^2)(1-y_{34}^2)} \right. \\ &\quad \times \cos \varphi + (1-x_{12}-x_{34})y_{12}y_{34} \\ &\quad \left. + \lambda^{1/2}(1, x_{14}, x_{23})(y_{12}+y_{34}) + 1-x_{12}-x_{34} \right); \end{aligned} \quad (\text{A.4})$$

It is worth noting that, in the present study, we use the notation nearly identical to that in [17], except for y_{ij} whose sign is opposite to that in [17]. Moreover, there are no here complications associated with nonzero masses of final-state leptons.

REFERENCES

1. CMS and LHCb Collab. (V. Khachatryan et al.), *Nature* (London, U.K.) **522**, 68 (2015).
2. ATLAS Collab. (M. Aaboud et al.), *Eur. Phys. J. C* **76**, 513 (2016).
3. LHCb Collab. (R. Aaij et al.), *Phys. Rev. Lett.* **118**, 191801 (2017).
4. R. Fleischer, R. Jaarsma, and G. Tetlalmatzi-Xolocotzi, *J. High Energy Phys.* **1705**, 156 (2017).
5. G. Buchalla, A. J. Buras, and M. E. Lautenbacher, *Rev. Mod. Phys.* **68**, 1125 (1996).
6. W. Buchmuller and D. Wyler, *Nucl. Phys. B* **268**, 621 (1986).
7. G. L. Kane, G. A. Ladinsky, and C.-P. Yuan, *Phys. Rev. D* **45**, 124 (1992).
8. CMS Collab. (V. Khachatryan et al.), *J. High Energy Phys.* **1702**, 28 (2017).
9. C. Bobeth, A. J. Buras, F. Krüger, and J. Urban, *Nucl. Phys. B* **630**, 87 (2002).
10. C. Bobeth, A. J. Buras, and T. Ewerth, *Nucl. Phys. B* **713**, 522 (2005).
11. S. Schilling, C. Greub, N. Salzmann and B. Tödtli, *Phys. Lett. B* **616**, 93 (2005).
12. T. Huber, E. Lunghi, M. Misiak, and D. Wyler, *Nucl. Phys. B* **740**, 105 (2006).
13. M. Misiak, A. Rehman, and M. Steinhauser, *Phys. Lett. B* **770**, 431 (2017).
14. D. Melikhov, *Eur. Phys. J. C* **4**, 1 (2002).
15. F. Krüger and D. Melikhov, *Phys. Rev. D* **67**, 034002 (2003).
16. T. Miyazaki and E. Takasugi, *Phys. Rev. D* **8**, 2051 (1973).
17. A. R. Barker, H. Huang, P. A. Toale, and J. Engle, *Phys. Rev. D* **67**, 033008 (2003).
18. LHCb Collab. (R. Aaij et al.), *Phys. Rev. Lett.* **110**, 211801 (2013).
19. LHCb Collab. (R. Aaij et al.), *J. High Energy Phys.* **1703**, 001 (2017).
20. D. Melikhov and B. Stech, *Phys. Rev. D* **62**, 014006 (2000).
21. Particle Data Group (C. Patrignani et al.), *Chin. Phys. C* **40**, 100001 (2016).
22. D. Melikhov and N. Nikitin, *Phys. Rev. D* **70**, 114028 (2004).
23. L. B. Okun, *Leptons and Quarks* (North-Holland, Amsterdam, 1984).
24. D. I. Melikhov, N. V. Nikitin, and K. S. Toms, *Phys. At. Nucl.* **68**, 1842 (2005).
25. D. Melikhov, *Phys. Rev. D* **53**, 2460 (1996).
26. D. Melikhov, *Phys. Rev. D* **56**, 7089 (1997).
27. D. I. Melikhov, private commun.
28. D. Guadagnoli, D. Melikhov, and M. Reboud, *Phys. Lett. B* **760**, 442 (2016).
29. D. Guadagnoli, *Mod. Phys. Lett. A* **32**, 1730006 (2017).
30. Y. Dinçer and L. M. Sehgal, *Phys. Lett. B* **556**, 169 (2003).
31. E. Byckling and K. Kajantie, *Particle Kinematics* (Wiley, London, 1973).